



**G. H. Raisoni
College of Engineering & Management**

Wagholi, Pune

Certificate

This is to certify that

Mr./Ms. Pratik Rajesh Jade

studying in Semester/Year First Year

Branch Artificial intelligence

Name of the Dept. F.Y.B.Tech

Section A

has satisfactorily completed the practical work of

subject Biomedical Engineering

during the academic year 2020-2021

Signature of Subject Teacher

Signature of Head of Department



INDEX PAGE



RAISONI GROUP
— A vision beyond —

Exp:1

Name of Experiment: Study of Human Physiology by Skeleton model.

Theory:

About Human Body

If we were to “break apart” the human body at the microscopic level, then the cell would constitute the most basic unit of life.

The average adult has somewhere between 30 – 40 trillion cells, and an estimated 242 billion new cells are produced every day. When a select group of cells with similar functions come together, it forms a tissue.

Tissues cumulate into organs, organ systems and eventually, an individual organism.

Cells -> Tissues -> Organs -> Organ System -> Organism

- Human Anatomy
- Human Physiology
 - Circulatory System
 - Digestive System
 - Reproductive System
 - Respiratory System
 - Nervous System
- Key Points About the Human Body

Human Anatomy

Skeleton

The human body exhibits a variety of movements from walking, bending and crawling to running, jumping and climbing. The framework that enables us to do all these activities is the skeleton. Humans have as much as 300 bones at birth. However, the bones start to fuse with age. At adulthood, the total number of bones is reduced to 206.

The skeleton also protects several vital organs such as the heart, lungs and the liver. Bones are attached to other bones through ligaments, a fibrous connective tissue.

Joints are points at which two bones meet. They enable a range of movements like rotation, abduction, adduction, protraction, retraction and more. Based on flexibility and mobility, joints can be further classified into movable joints and immovable joints. Movable joints are flexible while immovable joints (also called fixed joints) are non-flexible since the bones are fused.

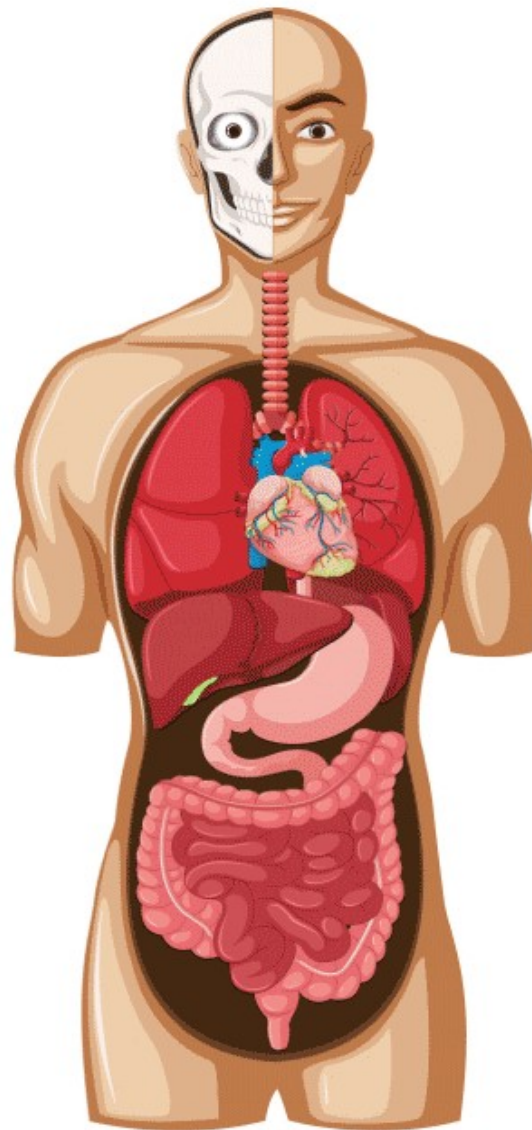
Muscles

Muscles are specialised tissues which assist the bones in locomotion. Muscles are attached to the bones through tendons. Movement of limbs happens due to the contraction and relaxation of the corresponding muscles present

in that region. Joints help in the flexibility of bones, but a bone cannot be bent or stretched until a muscle acts on it. In other words, the muscles attached to that bone pulls it to the direction of movement.

Furthermore, most movement involves muscles that work as a pair. For example, when we bend our arm, muscles in that region contract, become shorter and stiffer and pull the bones to the direction of movement. For relaxation (stretching), muscles in the opposite direction have to pull the bones towards it.

HUMAN ANATOMY



Human Anatomy is the scientific study of form and shapes of human beings

Muscles

Muscles are specialised tissues which assist the bones in locomotion. Muscles are attached to the bones through tendons. Movement of limbs happens due to the contraction and relaxation of the corresponding muscles present in that region. Joints help in the flexibility of bones, but a bone cannot be bent or stretched until a muscle acts on it. In other words, the muscles attached to that bone pulls it to the direction of movement.

Furthermore, most movement involves muscles that work as a pair. For example, when we bend our arm, muscles in that region contract, become shorter and stiffer and pull the bones to the direction of movement. For relaxation (stretching), muscles in the opposite direction have to pull the bones towards it.

List of Human Body Parts

- Human body parts comprise a head, neck and four limbs that are connected to a torso.
- Giving the body its shape is the skeleton, which is composed of cartilage and bone.
- Human body internal parts such as the lungs, heart, and brain, are enclosed within the skeletal system and are housed within the different internal body cavities.
- The spinal cord connects the brain with the rest of the body.

Human Body Structure

There are different cavities in the human body that house various organ systems.

1. The cranial cavity is the space within the skull, it protects the brain and other parts of the central nervous system.
2. The lungs are protected in the pleural cavity.
3. The abdominal cavity houses the intestines, liver and spleen.

Humans have evolved separately from other animals, but since we share a distant common ancestor, we mostly have a body plan that is similar to other organisms, with just the muscles and bones in different proportions.

For example, we might assume giraffes have more vertebrae in its neck than humans. No, despite being incredibly tall, giraffes have the same number of vertebrae, i.e. they also have seven vertebrae in their neck.

One of the most prominent characteristic features is the ability to use our hands, especially for tasks that require dexterity, such as writing, opening a bottle of water, opening a doorknob, etc.

This is the result of humans having ancestors that began walking on their hind limbs rather than using all four limbs. Most of our anatomical insight was gained through the dissection of corpses (cadavers), and for a long time, it was the only way we could gain anatomical knowledge about the human body. It was a rather grotesque affair, but it made up the bulk of medical literature for centuries. These days, technological innovation has made it possible to explore human anatomy at a microscopic level.

Even to this day, scientists are newly discovering organs that were previously overlooked or have been mistakenly identified as other existing tissues. In 2018, scientists had discovered a new, body-wide organ called the Interstitium that exists right under the skin.

Human Physiology

It is referred to the physical, mechanical, and biochemical function of humans. This connects health, medicine, and science in a way that studies how the human body acquaints itself to physical activity, stress, and diseases.

The person who is trained to study human physiology is called a physiologist. Claude Bernard is referred to as the father of Physiology for his exemplary research.

Read More: Physiology

Human Body Parts and their Functions

The list of human body parts vary as the standard definition of an organ is still up for debate. However, there are an estimated 79 organs identified to date. We also possess organs that have “lost” their function throughout our evolution. Such organs are called vestigial organs.

Some of these organs work together and form systems that are specialised to perform a specific function or a set of functions. Collectively, these are known as organ systems.

And out of these 79 organs, five are crucial for survival, and any damage to these five organs might result in termination of life. These five crucial human body parts are the brain, heart, liver, lungs and kidneys. Read on to explore more about these body parts and their functions in detail:

Circulatory System

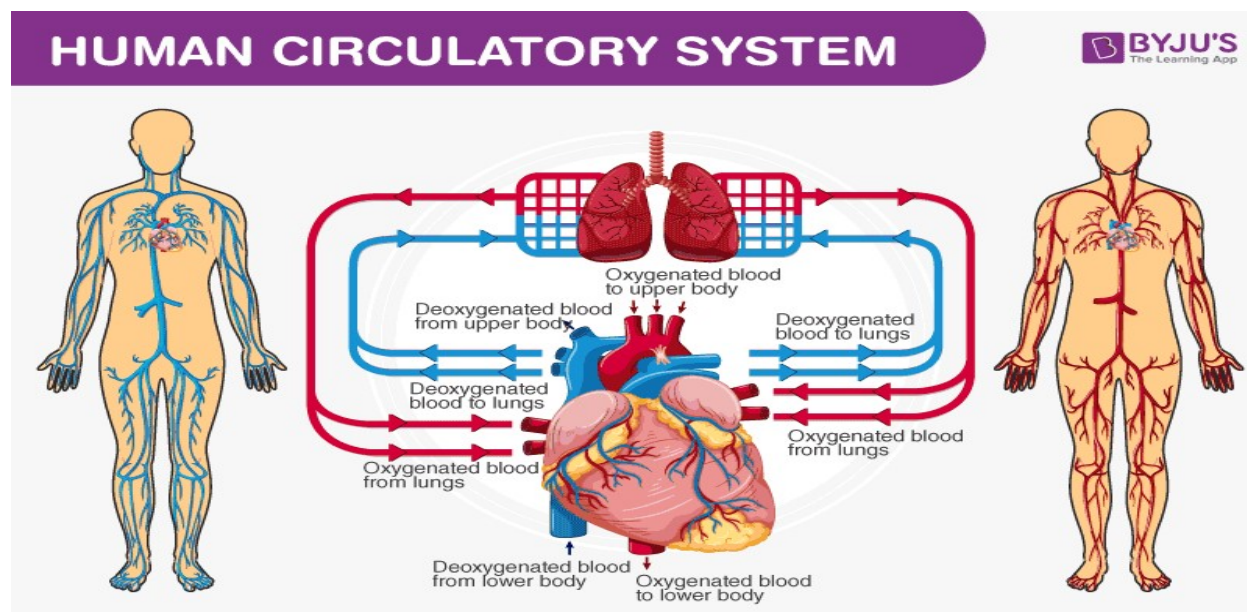
The **circulatory system** is also referred to as the cardiovascular system. It comprises the heart and all the blood vessels: arteries, capillaries, and veins. There are essentially two components of circulation, namely:

- Systemic circulation
- Pulmonary circulation

Diagram showing pulmonary (blue) and systemic circulation (red)

Besides these two, there is a third type of circulation called Coronary circulation. Because blood is the body's connective tissue, it helps to transport essential nutrients and minerals to the cells and waste byproducts away from it.

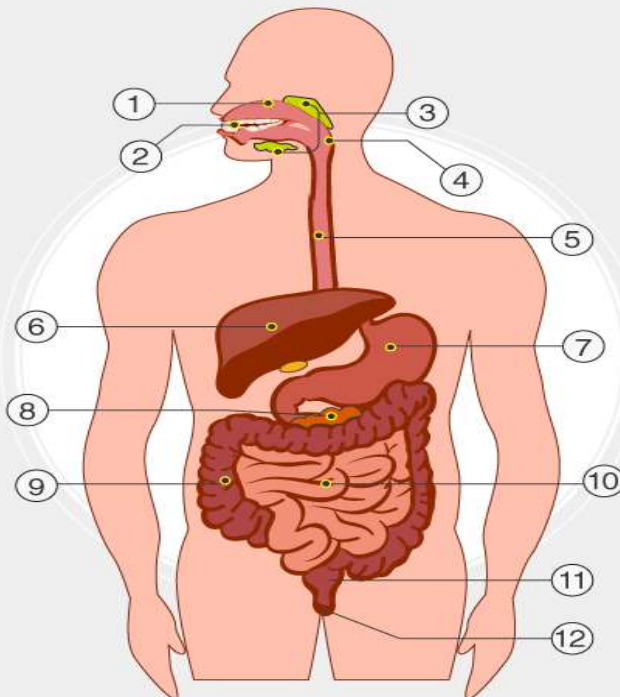
Hence, it is also known as the body's “transport system.” Anatomically, the **human heart** is similar to other vertebrate hearts in the animal kingdom and hence, is a homologous organ.



Digestive System

HUMAN DIGESTIVE SYSTEM

 BYJU'S
The Learning App



- | | | | |
|-------------------|--------------------|-------------------|------------|
| 1 Mouth | 2 Teeth | 3 Salivary glands | 4 Pharynx |
| 5 Esophagus | 6 Liver | 7 Stomach | 8 Pancreas |
| 9 Large intestine | 10 Small Intestine | 11 Rectum | 12 Anus |

© Byjus.com

A diagram of the human digestive system detailing various components

The digestive system breaks down food and assimilates nutrients into the body, which the body then uses for growth and cell repair.

The major components of the digestive system are:

- Mouth
- Teeth
- Tongue
- Oesophagus
- Stomach
- Liver
- Pancreas
- Gastrointestinal tract
- Small and large intestines
- Rectum

The process of digestion starts with mastication (chewing food). Then, the saliva mixes with food and forms a bolus, a small rounded mass that can be easily swallowed. Once swallowed, the food travels down the oesophagus and into the stomach. The stomach secretes strong acids and powerful enzymes that break the food down into a paste.

It then moves into the small intestine where the food is broken down even more because of the bile secreted by the liver and powerful, digestive enzymes from the pancreas. This is the stage at which nutrients are absorbed from the food.

The leftover materials (stool) then move on to the large intestine where it transforms from liquid to solid, as water is removed. Finally, it gets pushed into the rectum, ready to be eliminated from the body.

Exp:2

Name of Experiment: To study and measure the EEG signals

Theory:

1. Introduction

Whether students are attentive when learning significantly influences their learning outcomes. In traditional face-to-face instruction, teachers generally observe students' expressions to determine whether they are sufficiently attentive. However, this method is excessively subjective and consumes a significant amount of the teacher's energy. Furthermore, besides face-to-face instruction, students may engage in distance learning over the Internet, which further increases the difficulty of determining whether students are attentive. In all circumstances, the neurons in the human brain are ceaselessly active, emitting small amounts of electromagnetic waves. These electromagnetic waves are used as electroencephalography (EEG) signals. Without training, humans are generally unable to control fluctuations in their EEG signals. Therefore, the use of EEG signals to determine whether students are learning attentively is viable. Based on the frequency range, EEG signals can be divided into the following five wavebands [1]:

- α activity: electromagnetic waves ranging between 8 and 13 Hz in frequency, and between 30 and 50 μ V in amplitude. This type of periodic wave is produced in the parietal and occipital regions of the brain when in a state of consciousness, quiet, or at rest. When thinking, blinking, or otherwise stimulated, α waves disappear. This is known as an alpha block.
- β activity: electromagnetic waves ranging between 14 and 30 Hz in frequency, and between 5 and 20 μ V in amplitude. This type of activity occurs in the frontal region when people are conscious and alert. These waves are particularly apparent when a person is thinking or receiving sensory stimulation.
- θ activity: electromagnetic waves ranging between 4 and 7 Hz in frequency, with an amplitude of less than 30 μ V. This activity primarily occurs in the parietal and temporal regions of the brain. Such waves are produced when people experience emotional pressure, interruptions of consciousness, or deep physical relaxation.
- δ activity: electromagnetic waves ranging between 0.5 and 3 Hz in frequency, and between 100 and 200 μ V in amplitude. In a conscious state, most adults exhibit almost no δ activity; instead, this activity occurs when in a deep sleep, unconscious, anesthetized, or lacking oxygen.
- γ activity: electromagnetic waves ranging between 31 and 50 Hz in frequency, and between 5 and 10 μ V in amplitude. Recent studies have found that γ activity is related to selective attention. Other studies have also highlighted that this activity is related to cognition and perceptual activity.

Because various regions of the brain produce EEG signals, cerebral electromagnetic activity is traditionally collected using the international 10–20 electrode placement system (10–20 System), which involves attaching electrodes to 37 locations on the skull. Although this method facilitates

the observation of all EEG signal changes, practically applying this technique to students is extremely inconvenient and impractical. Because a person's emotions, mental state, and attentiveness are governed by various parts of the brain in the forehead region, observing the EEG signals from this area is a viable method for determining whether students are attentive. To facilitate the wearing of electrodes, this study adopted a commercialized mobile wireless EEG signal detection device for detecting and analyzing EEG signals of the frontal lobe. Because few previous studies have employed classrooms as the research environment, this study uses EEG signals as the medium to observe students' attentiveness during learning. The characteristics of EEG signals during states of attentiveness were identified by applying classifiers to the observed EEG data. The objective of this study was to successfully observe and identify whether students are attentive using simple EEG signal detection and classification. By employing the proposed system, teachers and the students themselves can assess their attentiveness during instruction, enabling both parties to implement necessary adjustments. Thus, the basic process of determining whether students are attentive involves classifying EEG signals. This study adopted a support vector machine (SVM) that produces excellent two-class results as the classifier. Mobile devices were employed to collect learners' EEG signals, which were then used to calculate various features. The effect that these features had on the classification performance was then analyzed. The remainder of this paper is organized as follows: Section 2 discusses relevant research; Section 3 describes the extracted features and the EEG classifier; Section 4 outlines the experimental results, and Section 5 presents the conclusions.

Go to:

2. Related Research

Beebe *et al.* investigated whether sleep disorders during puberty cause inattention and consequently affect learning. The results indicated greater θ activity when the subjects were inattentive [2]. Vidal *et al.* suggested the concept of brain-computer interface (BCI) technology [3,4], primarily regarding using BCI systems as communication tools between humans and the world, transforming detected EEG signals into commands, and realizing actions through hardware equipment. As published in *Neuroscience Letters*, Scherer *et al.* developed a system [5] for classifying EEG signals using Fisher's linear discriminant analysis (FLDA) and a virtual keyboard for spelling. This involved constructing a system based on the EEG signals produced when a person thought of the three directions down, left, and right. In 1977, researchers analyzed the power spectrum of EEG signals and found that it can reflect fluctuations in the level of alertness [6]. Scholars have also used EEG signals to evaluate mental exhaustion [7,8], identify feelings after listening to music [9] or observing various sports [10], assess emotions [11], control the movement of small mechanized vehicles, and alter the height of hospital beds.

Research regarding EEG signals, concentration, and learning remains immature because scholars and researchers have only recently begun exploring this field. A further motivation for such research is to facilitate long-distance learning [12,13]. Because actual face-to-face contact between teachers and students is impossible with long-distance learning, the difficulty of assessing students' learning state is greater than that with the face-to-face teaching method. Therefore, scholars and researchers have begun examining the relationship between EEG signals, learning, and concentration. In 2001, Gerlic *et al.* [14] observed alpha activity to examine the differences in EEG signals generated by beginner teachers compared to professional teachers, and by teaching courses

that employ textual materials compared to multimedia materials. The results showed that learning ability is better controlled under the instruction of professional teachers, and multimedia material more easily stimulates brain activity compared to textual material. Yaomanee *et al.* [15] identified locations on the scalp that are suitable for detecting attention related EEG signals. The study involved three experiments (*i.e.*, reading a book, locating 3D figures, and answering questionnaires) for determining whether the subjects were attentive. A two-minute piece of music was played to all subjects before the experiment to encourage relaxation, and any EEG signal changes during this period were observed. The results showed that α activity was slightly higher when the subjects were in a relaxed state, whereas β activity was greater when the subjects were attentive. Li *et al.* [13] developed an emotional learning system that was subsequently combined with the two classification methods of k -nearest neighbor (k NN) and naive Bayes. Students' emotions and attitudes were analyzed according to the alpha and theta activity-related EEG signal electrical potential collected from 13 locations using the previously mentioned classification methods to identify their level of attentiveness. The experiment results showed a maximum identification rate of 66.7%; however, the average rate was 44.4%. Li *et al.* [16] conducted EEG examinations using brain power-related tasks and asked the subjects to report their level of attentiveness. They employed k NN classification as the research method, and designed a system for instantly measuring people's level of attentiveness. The classification accuracy of the system was 57.3%. Belle *et al.* [17] employed EEG and electrocardiography (ECG) to compare their classification accuracy for attentiveness. The experiments involved the participants watching an interesting and tedious video clip for 20 min each before performing classification calculations using regression, C4.5, and random forest. The results of these methods for examining biological data show that the classification accuracy of EEG is 8.74% higher than that of ECG. This finding indicates that EEG is an appropriate technique for observation. In addition, EEG involves a substantial amount of data and is worthy of continued research and additional applications.

SVM is a supervised learning algorithm for solving binary classification problems that was proposed by Vapnik in 1995 [18]. SVM is generally applied to statistical classification and regression problems [19]. Cuingnet *et al.* [20] combined SVM and the Laplacian classification method to increase the ease of resolving cerebral image rendering. This technique can also be employed to render 3D images and images of the area between the two layers of the cerebral cortex. However, a comparison and classification of cerebral images obtained from 30 elderly subjects and 30 Alzheimer's patients indicated that cross-section cerebral images are identical to the images rendered using the technique described previously. Costantini *et al.* [21] applied SVM classification to EEG signals to design a BCI system capable of developing simple mathematical calculations or identifying the signals that indicate movement of the left or right hand. Jrad *et al.* [22] proposed using a weighted SVM to design a framework for classifying EEG signals. The results showed that a sensor weighting SVM (sw-SVM) can effectively classify datasets and error-related potential (ErrP) datasets. This method is also suitable for classifying the event-related potential (ERP) of small-scale training samples.

Go to:

3. Feature Extraction and EEG Classification

Although every person's attentiveness to the same learning content differs, and their EEG signal fluctuations vary, this study aims to identify the changes in EEG signals during attentive learning

under normal conditions by using convenient and simple methods. In a controlled learning environment, the influence (attentive or inattentive) that the experiment had on the students and EEG-related data was determined and analyzed. An SVM classifier was then employed to identify the classification information, thereby achieving the study objective.

Brainwave sensors were adopted to collect the subjects' EEG signals when learning. EEG sensing and data processing modules were then used to filter and prepare the collected data. The features of EEG signals after processing were separated into the two categories of attentive and inattentive, and employed as the SVM classifier training set. After optimizing the SVM classifier configurations, the classifier was used to instantly detect and identify the participants EEG data during instruction to assist teachers with assessing the students' attentiveness levels.

3.1. EEG Sensors

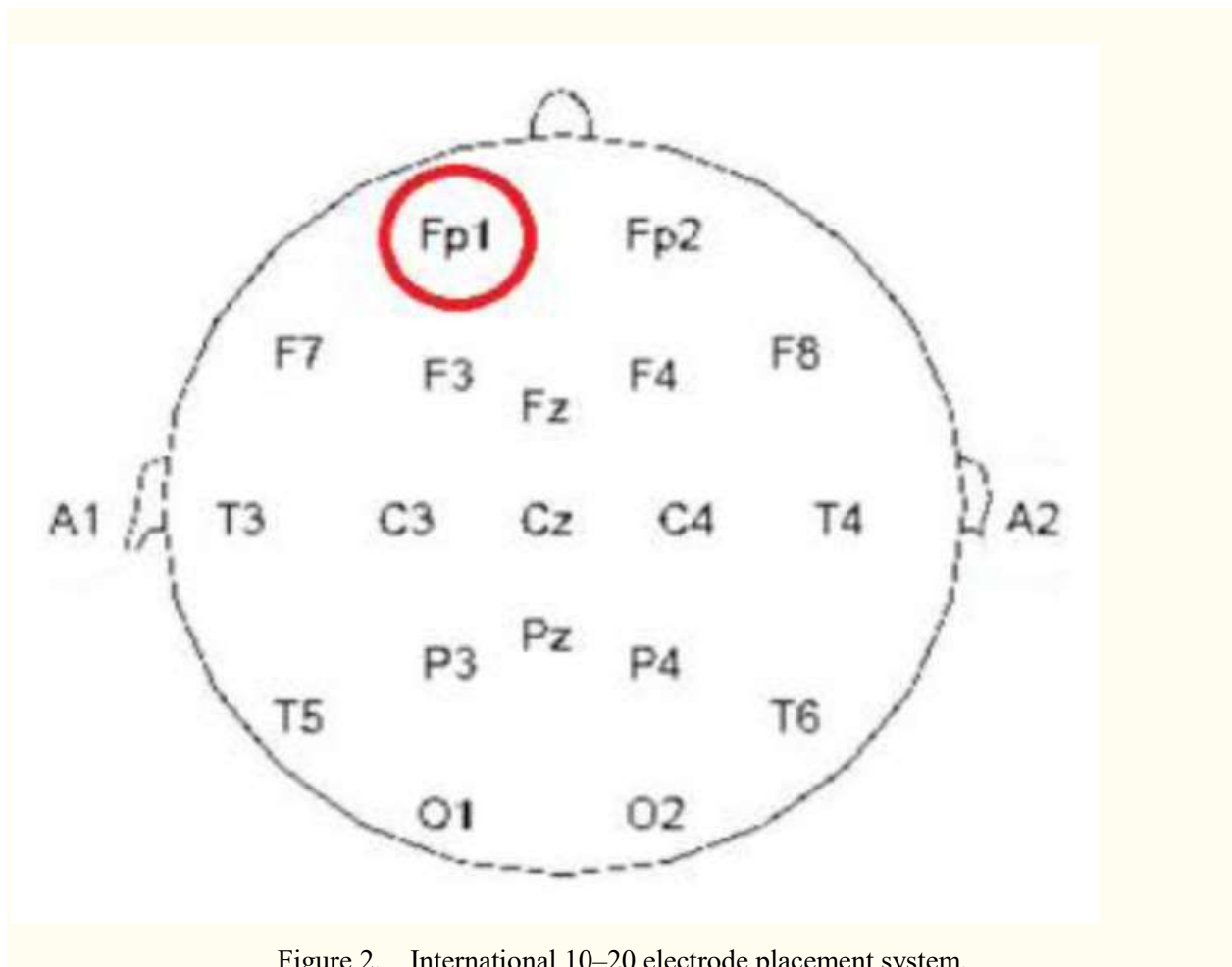
To facilitate within-classroom use by students, this study employed highly portable mobile brainwave sensors, as shown in [Figure 1](#). These brainwave sensors detected and digitized weak EEG signals produced by the brain and then wirelessly transmitted them to the hardware equipment. The EEG signal detection device employed for this study was MindSet, which features a single dry sensor. Ground and reference sensors were placed on the subjects' left ear. Wireless Bluetooth connectivity facilitated mobility. Sample rates as high as 512 Hz delivered raw signals in the alpha, beta, delta, gamma, and theta bands. The brainwave sensors use ThinkGear AM chip module technology to identify and digitize weak EEG signals, and can filter and extract electrical signals, such as the electrical waves produced by muscle movement, from the surrounding environment. The module chips collect, filter, augment, perform A/D conversions, process, and analyze EEG signals, before transmitting the processed and digitized EEG signals to the hardware equipment.



Figure 1.

The brainwave sensor and application method.

After a century of experimentation, experts in the field of neuroscience have defined the various areas that control corporal movement in the cerebrum. For example, the top of the cerebrum controls the limbs, and the posterior of the cerebrum controls sight. Because all areas of the cerebrum can produce EEG signals, electromagnetic waves are traditionally collected according to the international 10–20 electrode placement system (10–20 System), which involves placing 37 electrodes on the skull. Although this method facilitates observation of EEG signal changes, applying this technique to students is inconvenient and impractical. Because human emotions, mental states, and levels of attentiveness are controlled by the cerebral cortex in the forehead, detecting the EEG signals produced in this area of the brain is a viable method for determining whether students are inattentive. In this study, the brainwave sensors collected EEG signals from Fp1, as shown in [Figure 2](#). The sensor manufacturers placed the sensor at Fp1 because of the similarity between Fp1 and Fp2 signals and because this placement is similar to the mechanical design typically used for headphones. Generally, dry sensors are prone to environmental influences (e.g., motion artifacts); thus, errors exist in the detected signals. Although the sensor in the proposed identification system is a dry sensor, it is easy to wear and economic and, thus, can be extensively employed for teaching. Therefore, this study examined the feasibility of differentiating between attentiveness and inattentiveness based on EEG signals acquired using the proposed sensor.



[Figure 2.](#) International 10–20 electrode placement system.

3.2. Feature Extraction

EEG data were recorded at a sampling rate of 512 Hz with a 16-bit quantization level. To simplify the data processing method, EEG data were processed using a low-pass filter with a cut-off frequency of 50 Hz. A fast Fourier transform (FFT) was employed to transform a segment with 512 sampling points to the frequency domain. The segment was slid with 256 points overlapping the previous segment. Assuming $F(n)$ ($n = 1, 2, \dots, 512$) is the FFT result of a segment, the associated Power Spectral Density (PSD) is as follows:

$$P(n)=F(n)F^*(n)N \quad (1)$$

where $F^*(n)$ is the conjugate function of $F(n)$ and $N = 512$.

Five types of brainwaves exist in EEG signals, namely, α , β , δ , θ , and γ . However, research has identified that the waves most related to human mental states are α , β , δ , and θ . The energy value is summed according to the waveband distribution of the EEG signals to produce four features. Assuming that P_{freq} is the energy value of frequency $freq$, the features can be defined as follows:

$$E\alpha=\sum_{freq=813} P_{freq} \quad (2)$$

$$E\beta=\sum_{freq=1430} P_{freq} \quad (3)$$

$$E\theta=\sum_{freq=47} P_{freq} \quad (4)$$

$$E\delta=\sum_{freq=0.53} P_{freq} \quad (5)$$

In addition, according to previous research, definite interrelations exist between α and β activities. For example, α activity indicates that the brain is in a state of relaxation, whereas β activity is related to stimulation. In the study mentioned previously, to observe continuous changes in the mental state of the subjects, the ratio of α and β activities was used as the feature for assessing the level of mental attentiveness. This study produced the following feature value using the same principle:

$$R=E\alpha E\beta$$

(6)

where R is also a feature for determining whether students are attentive. Therefore, in this study, five features are extracted as the basis for classification. In this study, the EEG signal data of the test subjects was manually separated into attentive and inattentive, and used to determine the recognition accuracy rate after completing calculations and classifications using the classifier.

3.3. SVM Classifier

This study employed SVM classifiers with an excellent classification algorithm to separate EEG signals into the two categories of attentive and inattentive. Ideally, an SVM can identify a hyperplane that separates attentive and inattentive EEG signal data in its high-dimensional feature spaces. The basic concept of an SVM is as follows: Each sample in a set of training samples is matched to two categories before being reflected into a high-dimensional space using the Kernel function [24]. Subsequently, the SVM attempts to create a model and uses it to assign the samples

to a category. The model then constructs a separating hyperplane in the high-dimensional space (denoted using the solid red line in Figure 3, Old Space). On either side of the hyperplane, which divides the samples, parallel hyperplanes are located (denoted using dotted black lines in Figure 3, New Space). The SVM maximizes the distance between these two parallel hyperplanes. A greater distance or difference between parallel hyperplanes indicates a smaller total SVM error rate.

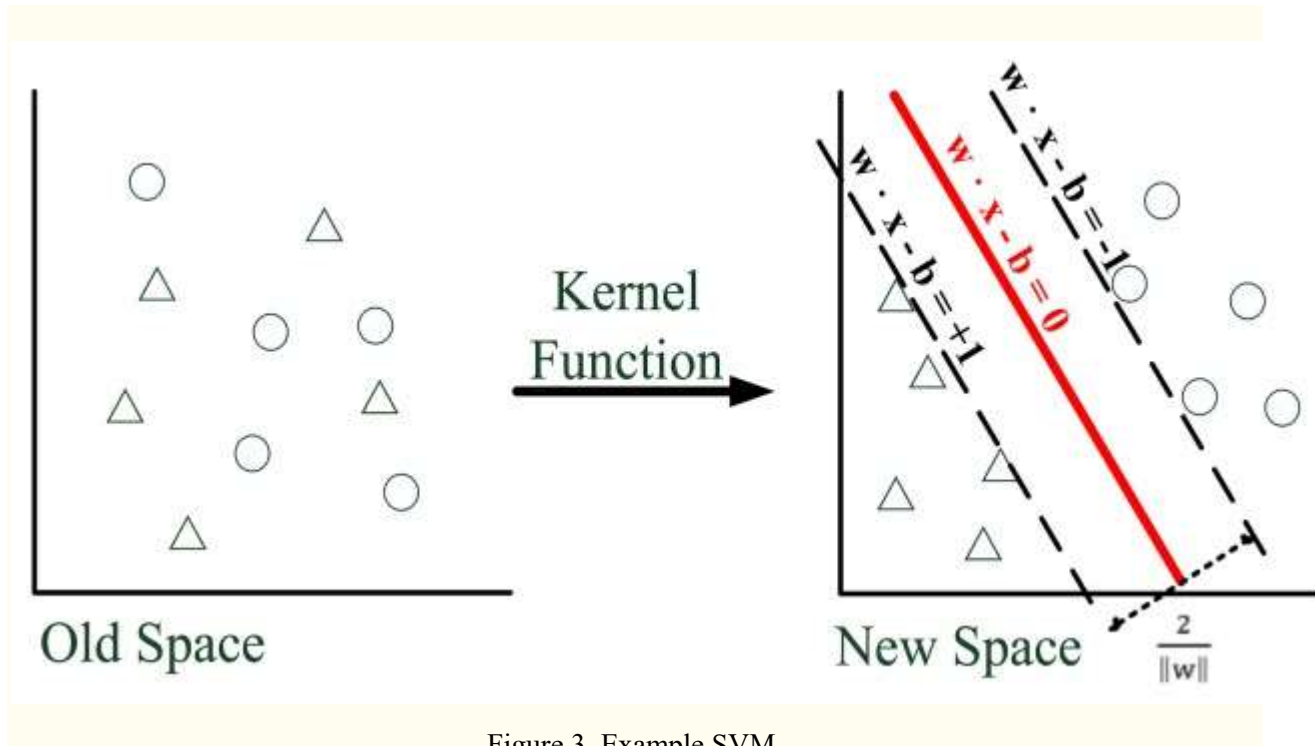


Figure 3. Example SVM.

According to the pretest results, polynomial kernel functions offer superior classification accuracy. Therefore, this study used a polynomial kernel function to project feature vectors into high-dimensional space before performing SVM calculations and classification. Furthermore, k -fold cross-validation was used to verify the recognition accuracy of the SVM classifier. Collected EEG signal data were randomly partitioned into non-repeating k subsample sets. One set was retained as validation data, and $k-1$ sets were used as training data. This process was repeated k times to determine the average value, which denoted the recognition accuracy rate.

Go to:

4. Experiments

Currently, an approved EEG signal database regarding attentiveness and inattentiveness is not available for analysis. The production of attentive and inattentive EEG signals when learning is an extremely difficult and complex process. This study designed a controlled environment and guided the subjects in producing the required EEG signal data. Based on the preliminary determination results and the subjects' subjective perceptions, these data were labeled according to category. Signals that were non-definitive were considered invalid. To accurately record the EEG signals of the test subjects and identify their level of attentiveness, in addition to recording their EEG signal

data during the experiment, their facial image and the surrounding sounds at the time of the experiment were also recorded to facilitate effective differentiation in post-experimental data analysis. The brainwave recording system is shown in [Figure 4](#), and the experimental environment is shown in [Figure 5](#).

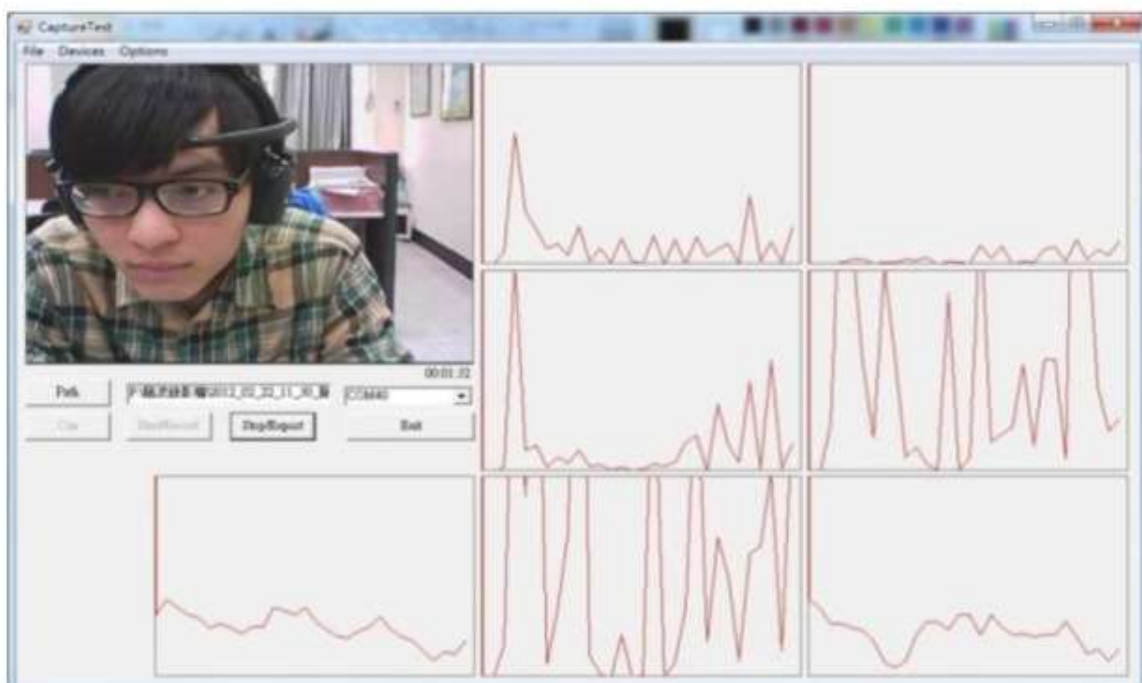


[Figure 4.](#) Real-time brainwave recording system.



[Figure 5.](#) Experimental environment.

4.1. Experiment Setting

This study recruited 24 test subjects (12 men and 12 women), with an average age of 25 years (the subjects' age ranged between 22 and 27 years). The hearing ability, mental state, and health conditions of the test subjects were normal. Furthermore, the test subjects had not undergone any EEG-related training. Since several studies maintain that the brainwave performance of males and females differs, this study aimed to design a gender dependant identification system. In the other words, two classifiers were developed for the proposed system and the EEG signals for male and female subjects were processed individually. Moreover, this study endeavored to design a system that does not require advanced collection of the users' EEG signal data. Thus, two classifiers (*i.e.*, one for male and one for female) capable of determining users' attentiveness and inattentiveness after training were developed.

To clearly identify the state of attentive EEG signals when students are learning, standard English class material was used as the experiment material for this study. The experiment involved the test subjects listening to English phrases and then answering related questions (question types: ordering the images, selecting answers based on illustrations, and multiple choice), to ensure that the test subjects could concentrate during the experiment. When the experiment was initiated, the test subjects were asked to wear the EEG sensor for 2 min to familiarize themselves with the sensor to prevent potential discomfort during use from influencing the accuracy of the experiment results. The volume of the speakers was also tested to ensure that the test subjects could conduct the experiment at the most appropriate volume. Each test subject was required to complete the English test under two scenarios. The first scenario was without interference, where the test subjects listened to English conversations before answering questions. The second scenario included the distraction of two people conversing while the test subjects listened to English conversations. They then answered questions and reported the content of the overheard conversation. The scenarios were designed to induce inattentive behavior when the test subjects completed the English examination. During the data collection experiment, 4291 unprocessed entries of EEG raw data were collected. The length of each datum was 1 s. The test subjects' conditions were manually determined. For the first and second scenario, the subjects were predetermined to be in an attentive and inattentive state, respectively. All collected data were examined, and the researchers and subjects reviewed video footage of the experiment together to determine whether the subject was in an attentive or inattentive state. If the subject was unsure of their mental state during the experiment, the particular datum was discarded. For example, in the first scenario, if the subject was unsure of whether they were attentive, the corresponding EEG signal was excluded. For the second scenario, if the subject was hesitant regarding whether they were inattentive, the corresponding brainwave was rejected. Once the test subjects' EEG data and data regarding their attentiveness were obtained, the feature values of attentive and inattentive EEG signals were marked. After eliminating ambiguous data, 4,289 and 2,674 attentive and inattentive EEG signal samples were obtained. To prevent the number of attentive and inattentive samples from affecting the classification accuracy of the classifier, 2,400 samples (1,200 samples from the male subjects and the others from the female subjects) each were randomly selected from the attentive and inattentive samples. Consequently, energy conversion was conducted on the original EEG signals to produce characteristics for classification.

For the SVM classifier, this study used two types of polynomial kernel functions and adjusted the cost parameter to analyze which combination of features can be used to obtain the optimum classification results. The polynomial kernel functions were as follows:

Polykernel:

$$K(x_i, x_j) = (x_i^T \cdot x_j + 1)^d \quad (7)$$

Normalized polykernel:

$$K(x_i, x_j) = (x_i^T \cdot x_j + 1)^d / \sqrt{x_i^T x_j + 1} \quad (8)$$

4.2. Experimental Results

This study originally employed a single feature for classification; however, the accuracy rate did not exceed 47%. Therefore, feature combinations were used as a basis for the classification system. First, the degree of influence that each feature has on the classification accuracy was determined. The analysis results are listed in [Table 1](#), which shows the average classification accuracy and the highest classification accuracy. To the classifiers for male and for female, the k value of k-fold was set as 5, which means 240 samples were used as testing samples.

Table 1.

The inference of classification accuracy using various features.

		$\alpha+\beta+\delta+\theta+R$	$\beta+\delta+\theta+R$	$\alpha+\delta+\theta+R$	$\alpha+\beta+\theta+R$	$\alpha+\beta+\delta+R$	$\alpha+\beta+\delta+\theta$
Average accuracy for training	PK	76.23	73.13	74.03	68.49	73.61	67.94
NPK	NPK	72.39	69.22	69.74	68.75	69.67	64.12
Average accuracy for k-fold	PK	75.87	72.36	74.16	68.63	73.45	67.25

		$\alpha+\beta+\delta+\theta+R$	$\beta+\delta+\theta+R$	$\alpha+\delta+\theta+R$	$\alpha+\beta+\theta+R$	$\alpha+\beta+\delta+R$	$\alpha+\beta+\delta+\theta$
	NPK	71.28	68.96	68.89	67.15	69.18	63.62
Highest accuracy for training	PK	77.96	74.14	75.25	69.43	74.81	68.02
	NPK	73.76	69.97	70.91	69.24	70.35	64.84
Highest accuracy for k -fold	PK	76.82	73.95	74.92	69.43	74.34	68.98
	NPK	73.83	70.42	69.73	68.38	70.12	64.46

PK: polykernel, NPK: normalized polykernel.

Table 1 shows that the polykernel classification accuracy rates all slightly exceed those of the normalized polykernel. Moreover, the results in Table 1 show that SVM can provide greater accuracy when all features are employed.

This study analyzed the accuracy rate for attentive and inattentive EEG signals when all features are used. If the classification accuracy rate of attentiveness is known as the attention rate (AR), the total number of attentive entries is called total attention (TA), and the correct classification of EEG signal data into the attentive category is labeled correct for attention (CA):

$$AR = (CATA \times 100)\% \quad (9)$$

Assuming that the classification accuracy rate of inattentiveness is called the inattention rate (IR), the total number of inattentive entries is known as the total inattention (TI), and the correct classification of EEG data into the inattentive category is labeled correct for inattention (CI).

$$IR = (CITI \times 100)\% \quad (10)$$

The number of TAs and TIs included in the sample was 2400 each. Table 2 shows the AR and IR of post-classification EEG data when the polykernel kernel function is employed. The data in Table 2 show that a greater cost parameter denotes a lower AR and a higher IR.

Table 2.

AR and IR when employing the poly kernel function.

Cost Parameter	Learning State	Training	k-Fold
1	AR (Attention)	90.43%	90.64%
	IR (Inattention)	54.26%	55.12%
10	AR (Attention)	90.48%	89.25%
	IR (Inattention)	57.67%	58.04%
50	AR (Attention)	87.23%	86.87%
	IR (Inattention)	59.84%	59.69%

4.3. Discussion

Table 1 indicates that the experiment data obtained in this study are unsuitable for normalized polykernel. Another inference based on Table 1 is that all five features have a significant influence on classification because removal of any feature causes a slight decline in both the highest and average classification accuracy rate compared to when all features are used. This indicates that each feature has a positive influence on the classification accuracy rate. However, according to the result of ANOVA (analysis of variance) testing, the contributions of features are different. Specifically, features δ and R exert the greatest influence on the classification accuracy. About the δ feature, the experiment result matches the conclusion in the literature [25] which stated that changes in delta activity are related to linguistic acquisition. Because the learning method in our experiment belongs to linguistic instruction, the δ feature value is an important basis for

classification. Although previous studies have contended that increased θ activity and reduced β activity respectively related to attention and inattention show minimal contributions from other wavebands, the experiment results of this study show that all features influence classification to some extent. The possible reason is that the limitations of a dry sensor for the detection location Fp1, only by using all wavebands can superior classification results be obtained.

Table 2 shows that the ratio of correct attentive classification entries (AR) was higher than that of correct inattentive classification entries (IR). Thus, this study infers that the EEG data obtained when the test subjects were attentive possess more identical or similar features, and are easier to recognize. This study also infers that the correct classification ratio of attentiveness is substantially higher than that of inattentiveness, which indicates that the collected attentive EEG data has more similar features and are more easily recognized. However, this does not indicate that inattentive EEG data are not easily recognized, but rather that many causes of inattentiveness exist. Therefore, a greater number of states are hidden within inattentiveness EEG data, necessitating further analysis for identification (e.g., the test subjects were required to multitask by listening to the content of the English sentences, listening to the additional conversations, and considering the content of these conversations). The IR values were not substantial at approximately 50%, which indicates that the system had a 50% probability of failing to detect students' inattentiveness. However, misdetection of students' attentiveness is less likely to affect their emotions during learning. A low AR results in the misjudgment that students are inattentive. If the system signals a warning, students may perceive interference with their studies. Furthermore, 2,400 test samples each were used to calculate AR and IR. However, the actual ratio of attentive to inattentive samples should be considered to determine the overall accuracy rate. For example, hypothesizing that the students were inattentive for 10% of the time during the experiment, the overall accuracy rate would be $AR \times 0.9 + IR \times 0.1$. Thus, when students are frequently inattentive, this study recommends adopting a system with a greater cost parameter for EEG classification. Conversely, a system with a lower cost parameter should be adopted when students are generally attentive.

Go to:

5. Conclusions

In traditional classrooms where teachers teach students face to face, the teacher can determine whether students are learning attentively based on their expressions and movements. However, for multimedia or distance learning, teachers experience greater difficulty determining whether students are learning attentively. Therefore, this study employed quantified EEG data to analyze students' learning status, thereby enabling teachers, students, and related personnel to understand whether students are attentive using scientific means. This allows teachers to adjust the teaching content, cultivate students' learning attitudes, and remind students to remain attentive. During the experiment, this study eliminated the features individually. The results showed that the optimum classification accuracy is achieved when five features are used simultaneously. However, the influence that each feature has on the classification accuracy differs. Of the features, the delta value causes the most significant changes, and can influence the classification accuracy by up to 6%. This has been rarely observed in previous studies. According to Penolazzi *et al.* [25], changes in delta activity are related to linguistic acquisition. Therefore, if the learning method belongs to linguistic instruction, the delta feature value would be an important basis for classification. In addition, a previous study has attested that theta and beta activity are not related to attentiveness;

however, this study employed more accurate sensing equipment and a greater number of locations when detecting EEG signals. Because of the limitations of a dry sensor for the detection location Fp1, only by using all wavebands can superior classification results be obtained.

The study results indicate that the state of attentiveness is a continuous phenomenon, and that the observation of data from a limited period is slightly superior to the classification accuracy of a single data entry. Furthermore, the EEG signals of attentiveness are easier to identify compared to those of inattentiveness; this is because the EEG signals of inattentiveness contain additional information. However, more unknown data or types of states may be extracted from the EEG signals of inattentiveness. The results also show that using polykernel kernel functions provides greater accuracy compared to using normalized polykernel kernel functions, which indicates that normalizing causes certain figures with a classification value to be obscured, resulting in a poorer classification performance. Currently, when using EEG signals without interference processing for classification, the accuracy rate for successfully detecting that the subject is inattentive is only 50%. EEG interference will be further examined in the future to enhance classification accuracy.

We hope that an immediate recognition system can be developed after EEG data is collected from additional test subjects. This would allow actual application in students' learning environments. Subjects of differing age groups and genders may produce varying EEG signals, which affect the classifier training effectiveness. Therefore, large-scale access of attentive and inattentive EEG signals is essential for future research. Numerous improvements can be made to the study's experimental collection of EEG signal data from subjects using English tests. This study anticipates developing additional methods for identifying subjects' attentiveness in the future. We hope that the methods mentioned in this study, for example, the k th NN classifier, artificial neural network, decision tree, and random forest, can be used to assess whether various classification methods improve the recognition accuracy rate of attentive EEG signals

Exp:3

Name of Experiment: To study and measure the ECG signals

Theory:

Abstract

Accurate detection of cardiac pathological events is an important part of electrocardiogram (ECG) evaluation and subsequent correct treatment of the patient. The paper introduces the results of a complex study, where various aspects of automatic classification of various heartbeat types have been addressed. Particularly, non-ischemic, ischemic (of two different grades) and subsequent ventricular premature beats were classified in this combination for the first time. ECGs recorded in rabbit isolated hearts under non-ischemic and ischemic conditions were used for analysis. Various morphological and spectral features (both commonly used and newly proposed) as well as classification models were tested on the same data set. It was found that: a) morphological features are generally more suitable than spectral ones; b) successful results (accuracy up to 98.3% and 96.2% for morphological and spectral features, respectively) can be achieved using features calculated without time-consuming delineation of QRS-T segment; c) use of reduced number of features (3 to 14 features) for model training allows achieving similar or even better performance as compared to the whole feature sets (10 to 29 features); d) k-nearest neighbors and support vector machine seem to be the most appropriate models (accuracy up to 98.6% and 93.5%, respectively).

Introduction

Cardiovascular diseases are currently the most common cause of death worldwide¹. Due to simplicity of the method, its non-invasive character and cheapness of the procedure, electrocardiography is still the most available and widely used method for the heart electrical activity examination. Electrocardiogram (ECG) reflects the electrical activity of the heart and gives a lot of information about heart function required for diagnosis of various diseases. Automatic analysis of ECG is a fundamental task in cardiac monitoring, especially in case of long-term monitoring, where large amount of data is recorded^{1·2}. Manual evaluation of such data is extremely time-consuming. Therefore, there is an effort to improve conventional and develop new methods for processing and analysing of electrocardiographic records.

Automatic classification of the heartbeats is one of the most important steps towards the identification of pathology using ECG. The correct choice of classification algorithm and features representing heartbeats is crucial for successful classification. Although many methods have been reported, their direct comparison is questionable due to their differences in: a) types of heartbeats being classified (normal vs ischemic^{3·4·5·6}, normal vs ventricular premature beats – VPBs^{7·8·9·10·11·12·13·14} etc.); b) ECG features (morphological^{4·5·7·15·16} spectral^{8·14} first-order or higher order statistics^{10·12} non-linear⁹, heart-vector projection¹⁷ etc.); c) classification models (discriminant function^{4·9} cluster analysis¹⁴, artificial neural network¹⁸, naive Bayes classifier¹³, support vector machine^{6·7} k-nearest neighbors^{5·11} etc.).

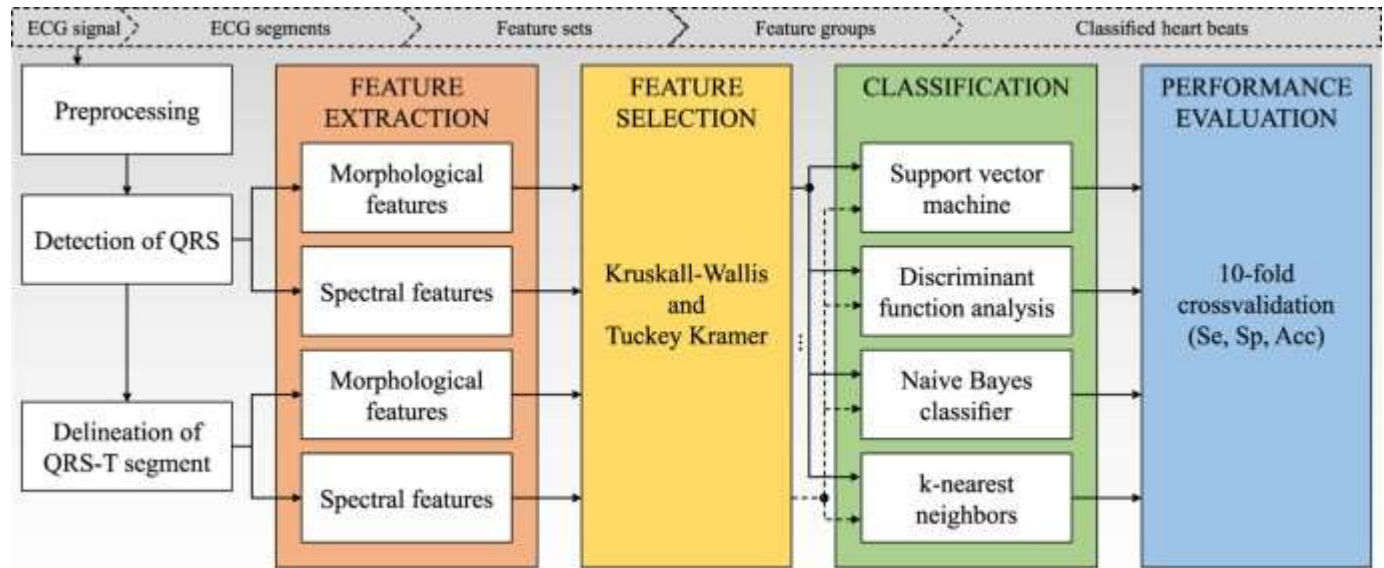
In this study, various approaches were applied for classification of heartbeats derived from experimental data recorded in rabbit isolated hearts under myocardial ischemia. In such experiments, the progression of myocardial ischemia and subsequent arrhythmias (ventricular premature beats – VPB, supraventricular premature beats, atrioventricular blockades, etc.) can be successfully evaluated. Four types of heartbeats were recognized: non-ischemic sinus, moderate ischemic, severe ischemic, and VPB. Moderate and severe ischemia as well as VPBs dramatically affect QRS complex morphology. On the other hand, QRS morphology in all these situations can be identical. It may result in reduced performance of classification due to decreased ability of the features to discriminate between these heartbeat types. Such phenomenon has not been covered by previous studies and, therefore, it is desirable to focus on it.

In this study, the most frequently used classification models (discriminant function analysis, naive Bayes classifier, support vector machine, and k-nearest neighbors – all with several different settings) and features (morphological and spectral) were tested on the same data set. Such approach allows reliable comparison of their suitability for classification. Besides commonly used voltage-related and interval-related features (such as ST segment deviation, QRS complex duration, etc.), new features based on area under various parts of ECG and its spectral representations obtained by four different approaches (fast Fourier transform, short-time Fourier transform, continuous wavelet transform, and Wigner-Ville distribution) were proposed. Finally, the effect of ECG segments definition (used for feature calculation) on classification performance was evaluated.

Methods

This section introduces proposed methods, including data acquisition, signal processing, feature extraction, feature number reduction, and classification (see Fig. 1).

Figure 1



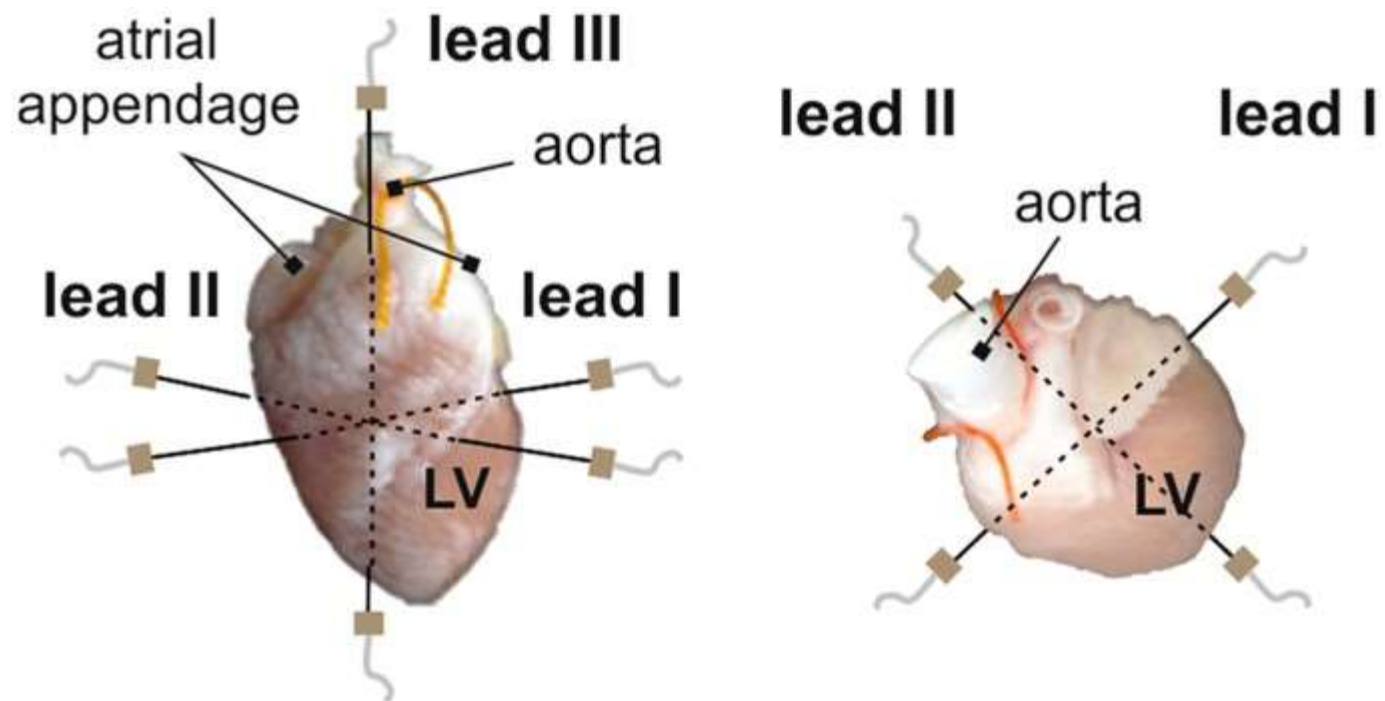
Complete scheme of electro gram processing and heartbeat classification.

Experimental data

The pathologies, that are classified in this work are not present in ECG signals from publicly available standard databases¹⁹⁻²⁰⁻²¹ therefore it was necessary to provide experimental ECG recordings. All experiments were carried out with respect to recommendations of the European Community Guide for the Care and Use of Laboratory Animals and according to the experimental protocol approved by the Committee for Ensuring the Welfare of Experimental Animals, Faculty of Medicine, Masaryk University.

Data were recorded during experiments focused on the effects of global ischemia on cardiac activity. The isolated hearts of 21 New Zealand rabbits perfused with Krebs-Henseleit solution (1.25 mM Ca^{2+} , 37°C) according to Langendorff with constant perfusion pressure (80 mmHg) were used in the study. During all experiments, ECGs were recorded by touch-less method using the orthogonal lead system which includes three pairs of Ag-AgCl disc electrodes (see Fig. 2). After stabilization period (30 min), global ischemia (10 min) followed by reperfusion (10 min) were carried out. More detailed information about experimental setup and data recording according to this protocol can be found in ref. ²². The sampling frequency of 2 kHz and 16 bit resolution were used, which are sufficient for further correct detection of QRS complex and delineation of QRS-T segment.

Figure 2



Front (left) and top (right) view of orthogonal system of electrodes. LV – left ventricle.
ECG processing

The low-frequency baseline wandering was suppressed by zero-phase Lynn's filter with cut-off frequency 0.5 Hz. Then, QRS complexes were automatically detected by algorithm based on

wavelet transformation using biorthogonal wavelet bior1.5. According to the detected QRS positions, 280 ms long QRS-T segments (part of a signal 30 ms before and 250 ms after QRS positions) were selected. Then, manual delineation of QRS-T was performed regarding three-lead ECG, including detection of the beginning of QRS, J point (QRS offset) and the end of T wave. After that, manual classification of heartbeats type (selected QRS-T) was performed by an expert. ECG from lead III was excluded from further analysis due to frequent occurrence of movement artefacts.

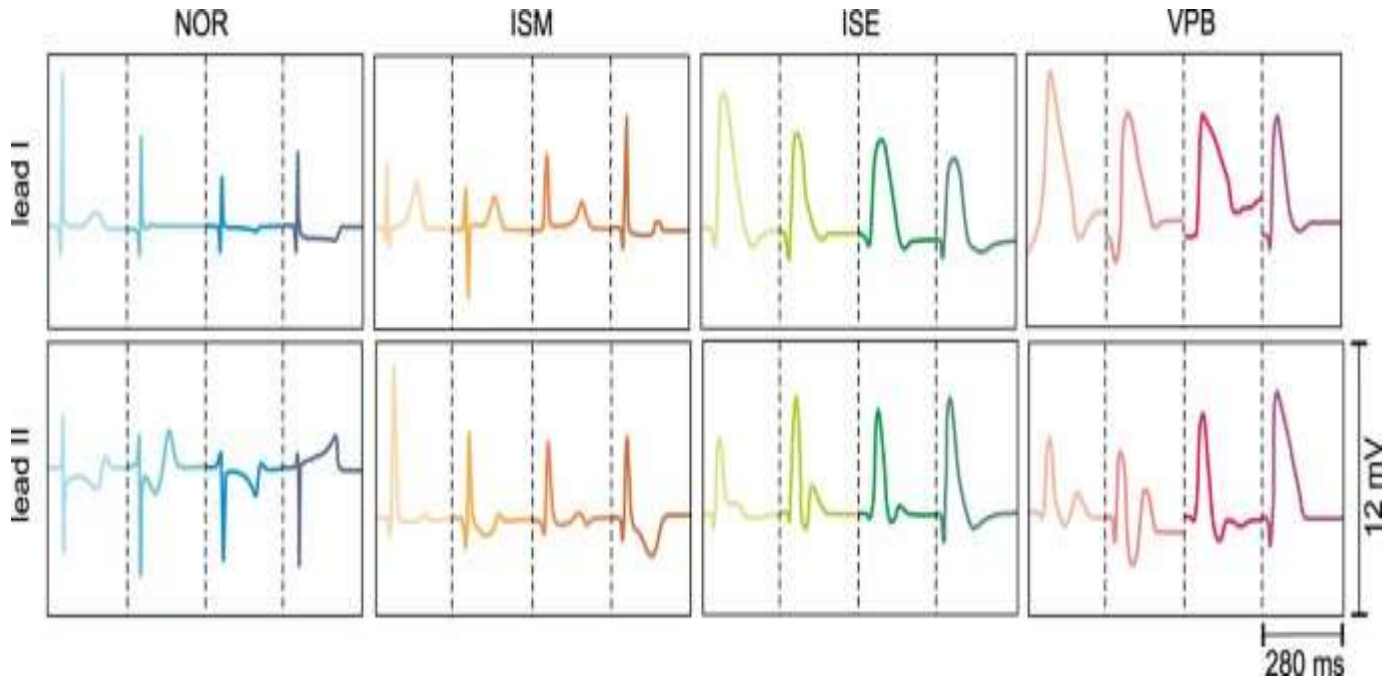
Heartbeat types

The narrow QRS complexes are related to electrical impulse generated by the sinus node and physiologically conducted through the ventricles. Myocardial ischemia and concomitant disorders lead to the reduced impulse propagation velocity and the changes in path of propagation due to presence of ectopic centres or blocked regions in the ventricles. These changes are reflected in ECG mainly as QRS widening, ST segment deviation (depression or elevation) and T wave polarity inversion, such as in case of ischemia manifestation in human ECG²³. Onset of the changes corresponds with the 3rd–5th minute of ischemic period and their magnitude depends on severity of myocardial ischemia. Therefore, four types of heartbeats with different morphology were classified in this study:

- non-ischemic (NOR) selected from stabilization period,
- VPBs selected from ischemic period,
- moderate ischemic beats (ISM) selected from ECG recorded in the 5th minute of ischemia, where only slight changes are characteristic for ECG morphology,
- severe ischemic beats (ISE) selected from ECG recorded in the 10th minute of ischemia, where the most prominent changes in ECG morphology are present.

Totally more than 260 000 heartbeats were labelled. However, only 172 VPBs were found in the records. Therefore, 220 representatives from each group (NOR, ISM and ISE) were selected to reduce the imbalance between classes and to provide sufficiently large data set for successful classification at the same time. In Fig. 3, all types of QRS-T segments selected from four different experiments are shown. It is evident, that NOR and ISM from lead I as well as ISE and VPB from leads I and II are quite similar. On the contrary, there are significant differences between beats from the middle (ISM) and the end (ISE) of ischemic period on one side and ISM and VPB on the other side. Besides mentioned inter-class differences, the intra-class variability (mainly regarding R peak deviation) is quite high.

Figure 3



Types of classified QRS-T segments. Segments from four different experiments are shown in each group. NOR, ISM, ISE, VPB – non-ischemic, moderate and severe ischemic beats and ventricular premature beats, respectively.

Features calculation

Commonly used (e.g refs [6](#), [10](#), [14](#) and [15](#)) and some newly proposed morphological and spectral features were calculated from each selected QRS-T segment.

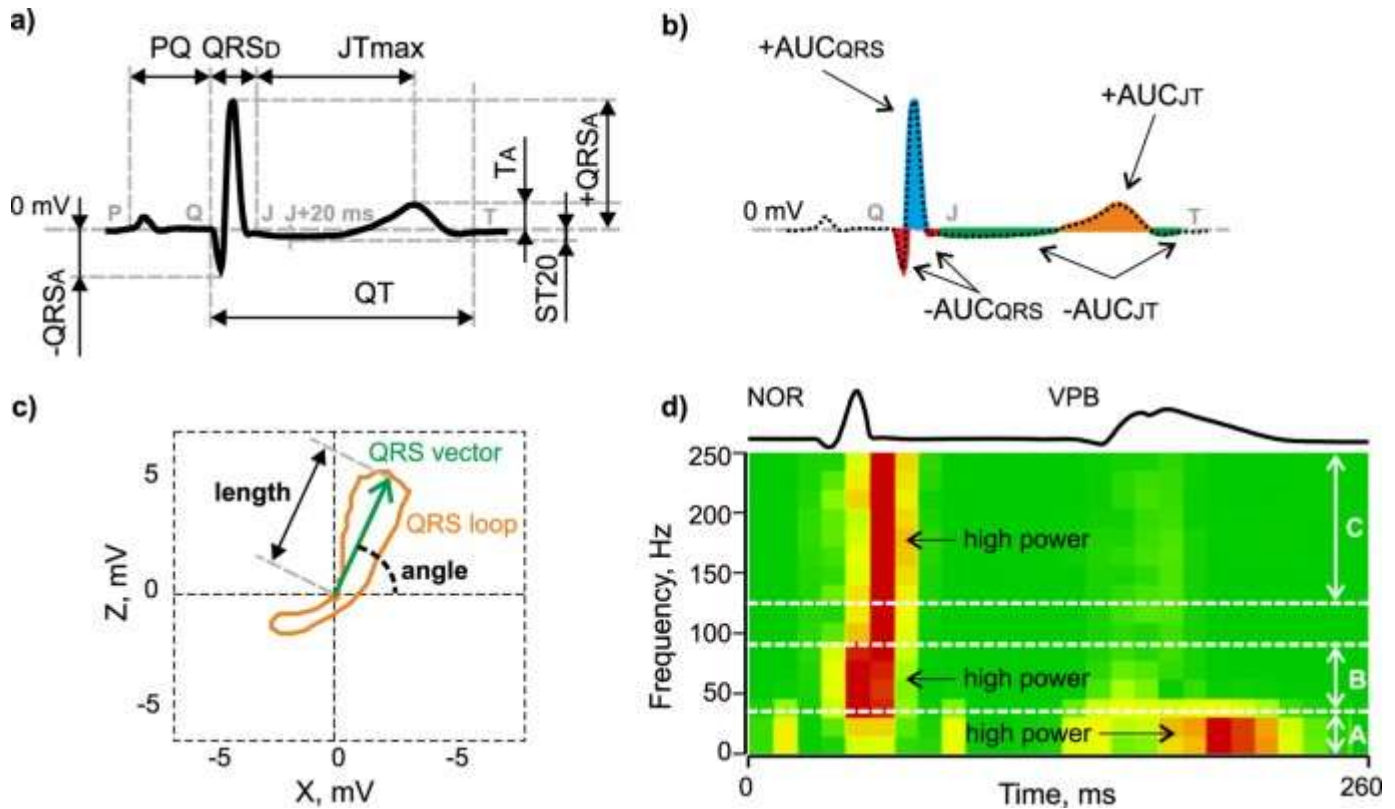
Morphological features: calculation from QRS-T obtained from ECG delineation

Total 71 features representing the ECG morphology were calculated from the segments selected from lead I and lead II based on the results of previous delineation (QRS onset, QRS offset (J point) and T wave offset).

First type of features represents *interval* (QRS, QT and ST-T duration) and *voltage* (e.g. maximal absolute, positive and negative deviation of QRS, maximal deviation of ST-T interval, deviation of ST segment 20 ms after QRS offset) characteristics of QRS-T. Illustration of selected features from this group is in Fig. [1a](#).

Second type of features describes *areas under* (AUC) various *parts* of QRS-T (e.g. AUC of the whole QRS-T, QRS and of only negative part of ST-T interval). Additionally, values of all AUC based features relative to AUC_{qrst} and positive to negative AUC ratios were calculated. Examples of this type of features are shown in Fig. [4b](#).

Figure 4



Selected features definition: (a) interval (QRS_D, QT, PQ, and JTmax represent the duration of QRS complex, QT interval, PQ interval, and segment between J point and maximal deviation of T wave, respectively) and voltage (+QRSA_A, -QRSA_A, T_A, and ST20 represent maximal positive deviation of QRS, maximal negative deviation of QRS, maximal deviation of ST-T interval, and deviation of ST segment 20 ms after QRS offset, respectively) characteristics of ECG; (b) areas under various parts of QRS-T (-AUC_{QRS}, +AUC_{QRS}, -AUC_{JT}, and +AUC_{JT} represent area under negative and positive part of QRS and negative and positive part of ST-T interval, respectively); (c) 2D QRS loop parameters (length and angle of maximal electrical vector of QRS in horizontal plane); (d) spectrogram of QRS used for calculation of (sum of frequency power (normalized for each frequency component separately - created by [28](#)) in three bands (A – 0–35 Hz, B – 35–90 Hz and C – 125–250 Hz); NOR, VPB - normal and ventricular premature beats, respectively.

The last type of features was calculated from 2D QRS and ST-T loops in horizontal plane: angle and length of maximal electrical vector separately for each loop. Examples of selected features are shown in Fig. 4c.

Interval characteristics and 2D loops features (total 7 features) were calculated using both leads together; other 32 features were derived for each lead separately.

Morphological features: calculation from segments obtained from R peak detection

Total 44 features were calculated from the segments obtained from R peak positions. These features do not depend on manual delineation procedure. Thus, their extraction is easier, faster and more objective than in previous case.

The first type of features represents *value* and *position* of maximum and minimum deviation of the whole 280 ms long QRS-T. Other features were computed as a difference between the deviations and as a time interval between their positions.

The second type of features is based on *AUC* calculated from the segments defined as $\langle R-t, R+t \rangle$, where R is the position of detected R peak and $t = 40$ ms, 60 ms or 100 ms. Values of t were chosen according to RR, QRS and QT intervals reaching in stabilization 344 ± 46 ms, 24 ± 4 ms and 175 ± 22 ms, respectively. Thus, the segments selected using different t contain QRS, QRS with adjacent ST or almost the whole QRS-T, respectively. Corresponding features include information about different parts of QRS-T, which may affect their discriminating ability and the performance of heartbeat classification. Under ischemia, RR and QRS are prolonged, whereas QT is shortened. Hence, selected segments do not contain the parts of adjacent heartbeats (even in case of the highest t), which is important for accurate features calculation.

AUC was also calculated from the whole 280 ms long QRS-T segments containing QRS-T and a short part of isoline after T wave and from negative and positive parts of the segments separately. Relative values and ratios of AUC features were calculated, too.

Spectral features: calculation from QRS obtained from ECG delineation

Total number of 24 features representing the spectrum of QRS was calculated from both leads (12 features for each lead). QRS were selected based on the manually detected QRS onsets and J points.

The first type of features was computed from spectrum obtained by *fast Fourier transform* (FFT) as the sum of particular components in three frequency bands commonly used for analysis of conventional and high-frequency QRS¹⁹: 0–35 Hz, 35–90 Hz and 125–250 Hz.

The second type was defined as mean, median and maximum of spectrogram computed by *short-time Fourier transform* (STFT). Only non-zero frequency components were included in calculations.

The third type of features was extracted in time-scale domain by *continuous wavelet transform* (CWT) performed using symlet wavelet sym2 at all integer scales from 1 to 32. Besides suitability for CWT, sym2 is symmetrical and allows achieving good results in case of noisy signals²⁴⁻²⁵⁻²⁶. Selected scales correspond to frequency range of the signal. The first two features were calculated as mean and maximum of CWT matrix. The third feature was found as a mean correlation between QRS and scaled versions of the mother wavelet placed in such a way that the highest correlation was obtained. On the contrary, the last feature was represented by mean correlation between QRS and differently placed wavelet scaled in such a way that the highest correlation was obtained.

The last features group was calculated from *Wigner-Ville distribution* of QRS. The features were calculated as a maximum and mean value of QRS distribution in the frequency range 0–500 Hz.

Spectral features: calculation from segments obtained from R peak detection

Total 24 features representing ECG spectrum were calculated from each type of segments defined as $\langle R-t, R+t \rangle$, where $t = 20$ ms, 30 ms or 50 ms. As compared to morphological features, narrower boundaries were set in order to select segments containing mainly QRS (narrow in case of non-ischemic condition or prolonged one in case of ISE or VPB). This is in agreement with well known approach, where spectral content of QRS complex (not ST-T) is used to assess myocardial ischemia in electrocardiographic signals²⁷. Generally, the features were computed by similar way as in previous section. Selected features are shown in Fig. 4d.

Features number reduction

Training of classification model using high-dimensional feature set may lead to model overfitting²⁹. Therefore, so called filter method (e.g. refs [29](#) and [30](#)) was applied to select only the most informative features showing statistically significant differences among particular classification groups. At first, the Shapiro-Wilk test was used to reveal data distribution. Then, non-parametric Kruskal-Wallis test ($\alpha = 0.05$) followed by Tukey-Kramer post-hoc test were used to compare features from particular groups and indicate those suitable for discrimination between various heartbeat types. Only features with significant differences between all pairs of classification groups were used for further analysis.

Automatic classification

Four models (with various settings) were used for automatic heartbeat classification based on selected features^{[29](#), [31](#), [32](#)}:

- discriminant function analysis (DFA) with linear and quadratic function,
- naive Bayes (NB) classifier with Gaussian kernel and kernel density function estimation,
- support vector machine (SVM) (one-vs-all approach for multiclass approach) of general type and with radial basis function (RBF),
- k-nearest neighbors (k-NN) with different k value ($k = 1, 5, 10$).

Selected models are widely used for heartbeat classification (see below). Moreover, the models represent different types of classifiers^{[32](#)}: a) supervised parametric (DFA and NB); b) supervised non-parametric (SVM); c) non-parametric algorithm based on instance learning (k-NN).

Training and testing of all classifiers were performed using 10-fold cross-validation approach³¹. Standardized features were used as an input to classification models. Common standardization procedure (e.g. ref. ³³) of training and testing data was performed for each fold separately, based on statistical measures (mean and standard deviation) calculated from training instances.

Classification performance of each approach was evaluated by mean overall accuracy (Acc), where Acc of particular validation folds was defined as a number of correctly classified heartbeats in all groups related to their total number. Sensitivity (Se) and specificity (Sp) were also calculated for more detailed performance analysis³⁴.

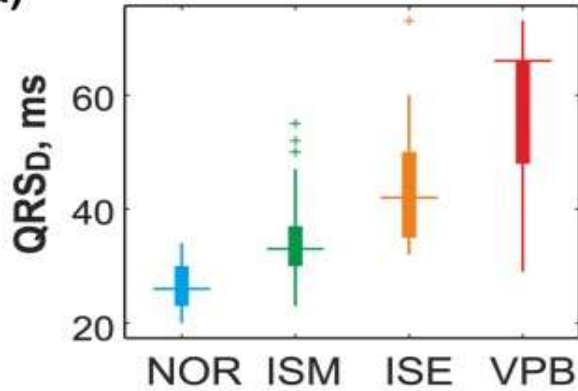
Results and Discussion

Selected classification features

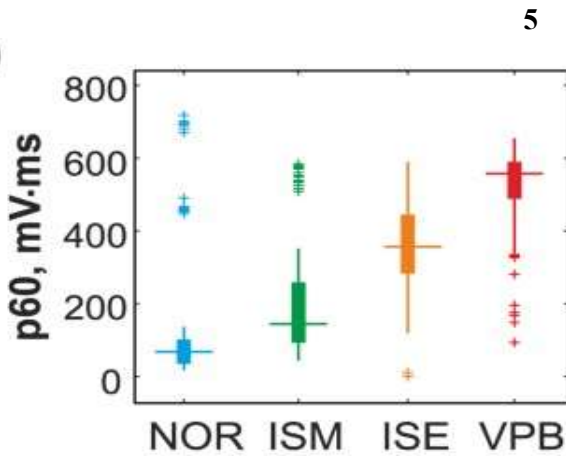
Based on the post-hoc test results, only the most informative features were chosen from the whole data set to represent QRS-T segments. Total number of 26, 24, 10, and 29 features were selected from morphological group obtained from ECG delineation and R peak detection and spectral group obtained from manual delineation and automatic R peak detection, respectively. Distribution of four selected features in particular classification groups is shown in Fig. 5.

Figure

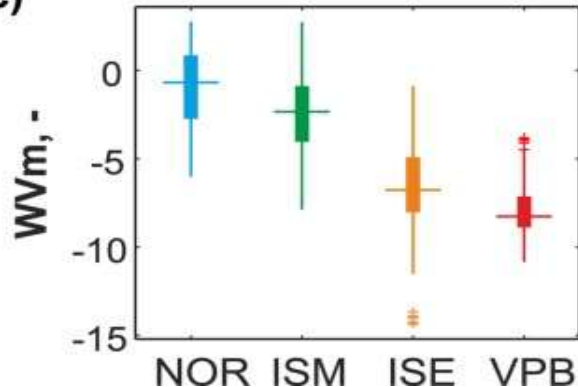
a)



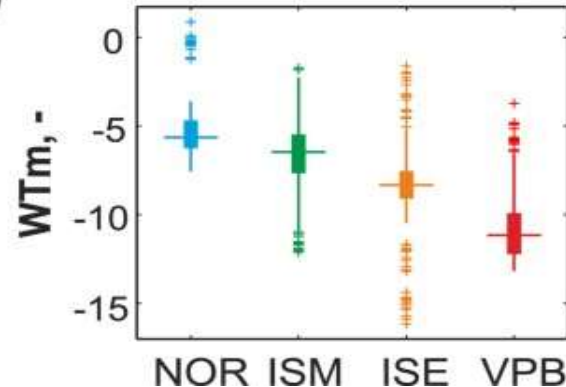
b)



c)



d)



Distribution of selected features with significantly different values among all types of heartbeats confirmed by statistical analysis ($p < 0.05$): **(a)** QRS complex duration (QRS_D), **(b)** area under segment selected as a part of ECG 60 ms before to 60 ms after R peak position ($p60$), **(c)** mean value of QRS in Wigner-Ville distribution within frequency range 0–500 Hz (WVm), **(d)** mean of continuous wavelet representation of QRS complex (WTm).

For more detailed evaluation of suitability of particular features for heartbeat classification, main feature groups were additionally divided into subgroups according to their characteristics as follows:

- 26 morphological features obtained from delineation (MorphD) were divided into 5 sets: CommonD (interval and voltage-based characteristics, $n = 3$), LoopD (features from 2D loops, $n = 2$), AreaD (general AUC based features, $n = 9$), AreaDa (AUC based features calculated from absolute values of the segments, $n = 5$), and AreaDr (relative AUC based features, $n = 7$);
- 24 morphological features obtained from R peak detection (MorphR) were divided into 3 subgroups: CommonR (interval and voltage-based features, $n = 3$), AreaR (general AUC based features, $n = 16$) and AreaRa (AUC based features calculated from absolute values of the segments, $n = 5$);
- 10 spectral features obtained from delineation (SpectralD) were not divided because of low number of features;
- 29 spectral features obtained from R peak detection (SpectralR) were divided into 3 subgroups according to t used for segments definition (see above): S20 ($n = 6$), S30 ($n = 9$) and S50 ($n = 14$) for $t = 20$ ms, 30 ms and 50 ms, respectively.

Exp:4

Name of Experiment: To study and measure the EMG signals

Theory:

Introduction

Biomedical signal means a collective electrical signal acquired from any organ that represents a physical variable of interest. This signal is normally a function of time and is describable in terms of its amplitude, frequency and phase. The EMG signal is a biomedical signal that measures electrical currents generated in muscles during its contraction representing neuromuscular activities. The nervous system always controls the muscle activity (contraction/relaxation). Hence, the EMG signal is a complicated signal, which is controlled by the nervous system and is dependent on the anatomical and physiological properties of muscles. EMG signal acquires noise while traveling through different tissues. Moreover, the EMG detector, particularly if it is at the surface of the skin, collects signals from different motor units at a time which may generate interaction of different signals. Detection of EMG signals with powerful and advance methodologies is becoming a very important requirement in biomedical engineering. The main reason for the interest in EMG signal analysis is in clinical diagnosis and biomedical applications. The field of management and rehabilitation of motor disability is identified as one of the important application areas. The shapes and firing rates of Motor Unit Action Potentials (MUAPs) in EMG signals provide an important source of information for the diagnosis of neuromuscular disorders. Once appropriate algorithms and methods for EMG signal analysis are readily available, the nature and characteristics of the signal can be properly understood and hardware implementations can be made for various EMG signal related applications.

So far, research and extensive efforts have been made in the area, developing better algorithms, upgrading existing methodologies, improving detection techniques to reduce noise, and to acquire accurate EMG signals. Few hardware implementations have been done for prosthetic hand control, grasp recognition, and human-machine interaction. It is quite important to carry out an investigation to classify the actual problems of EMG signals analysis and justify the accepted measures.

The technology of EMG recording is relatively new. There are still limitations in detection and characterization of existing nonlinearities in the surface electromyography (sEMG, a special technique for studying muscle signals) signal, estimation of the phase, acquiring exact information due to derivation from normality (1, 2) Traditional system reconstruction algorithms have various limitations and considerable computational complexity and many show high variance (1). Recent advances in technologies of signal processing and mathematical models have made it practical to develop advanced EMG detection and analysis techniques. Various mathematical techniques and Artificial Intelligence (AI) have received extensive attraction. Mathematical models include wavelet transform, time-frequency approaches, Fourier transform, Wigner-Ville Distribution (WVD), statistical measures, and higher-order statistics. AI approaches towards signal recognition include Artificial Neural Networks (ANN), dynamic recurrent neural networks (DRNN), and fuzzy logic system. Genetic Algorithm (GA) has also been applied in evolvable hardware chip for the mapping of EMG inputs to desired hand actions.

Wavelet transform is well suited to non-stationary signals like EMG. Time-frequency approach using WVD in hardware could allow for a real-time instrument that can be used for specific motor unit training in biofeedback situations. Higher-order statistical (HOS) methods may be used for analyzing the EMG signal due to the unique properties of HOS applied to random time series. The bispectrum or third-order spectrum has the advantage of suppressing Gaussian noise.

This paper firstly gives a brief explanation about EMG signal and a short historical background of EMG signal analysis. This is followed by highlighting the up-to-date detection, decomposition, processing, and classification methods of EMG signal along with a comparison study. Finally, some hardware implementations and applications of EMG have been discussed.

Go to:

Materials and Methods

EMG: anatomical and physiological background

EMG stands for electromyography. It is the study of muscle electrical signals. EMG is sometimes referred to as myoelectric activity. Muscle tissue conducts electrical potentials similar to the way nerves do and the name given to these electrical signals is the muscle action potential. Surface EMG is a method of recording the information present in these muscle action potentials. When detecting and recording the EMG signal, there are two main issues of concern that influence the fidelity of the signal. The first is the signal-to-noise ratio. That is, the ratio of the energy in the EMG signals to the energy in the noise signal. In general, noise is defined as electrical signals that are not part of the desired EMG signal. The other issue is the distortion of the signal, meaning that the relative contribution of any frequency component in the EMG signal should not be altered. Two types of electrodes have been used to acquire muscle signal: invasive electrode and non-invasive electrode. When EMG is acquired from electrodes mounted directly on the skin, the signal is a composite of all the muscle fiber action potentials occurring in the muscles underlying the skin. These action potentials occur at random intervals. So at any one moment, the EMG signal may be either positive or negative voltage. Individual muscle fiber action potentials are sometimes acquired using wire or needle electrodes placed directly in the muscle. The combination of the muscle fiber action potentials from all the muscle fibers of a single motor unit is the motor unit action potential (MUAP) which can be detected by a skin surface electrode (non-invasive) located near this field, or by a needle electrode (invasive) inserted in the muscle (3). Equation 1 shows a simple model of the EMG signal:

$$x(n) = \sum_{r=0}^{N-1} h(r)e(n-r) + w(n) \quad (1)$$

where, $x(n)$, modeled EMG signal, $e(n)$, point processed, represents the firing impulse, $h(r)$, represents the MUAP, $w(n)$, zero mean additive white Gaussian noise and N is the number of motor unit firings.

The signal is picked up at the electrode and amplified. Typically, a differential amplifier is used as a first stage amplifier. Additional amplification stages may follow. Before being displayed or stored, the signal can be processed to eliminate low-frequency or high-frequency noise, or other

possible artifacts. Frequently, the user is interested in the amplitude of the signal. Consequently, the signal is frequently rectified and averaged in some format to indicate EMG amplitude.

The nervous system is both the controlling and communications system of the body. This system consists of a large number of excitable connected cells called neurons that communicate with different parts of the body by means of electrical signals, which are rapid and specific. The nervous system consists of three main parts: the brain, the spinal cord and the peripheral nerves. The neurons are the basic structural unit of the nervous system and vary considerably in size and shape. Neurons are highly specialized cells that conduct messages in the form of nerve impulses from one part of the body to another.

A muscle is composed of bundles of specialized cells capable of contraction and relaxation. The primary function of these specialized cells is to generate forces, movements and the ability to communicate such as speech or writing or other modes of expression. Muscle tissue has extensibility and elasticity. It has the ability to receive and respond to stimuli and can be shortened or contracted. Muscle tissue has four key functions: producing motion, moving substance within the body, providing stabilization, and generating heat. Three types of muscle tissue can be identified on the basis of structure, contractile properties, and control mechanisms: (i) skeletal muscle, (ii) smooth muscle, and (iii) cardiac muscle. The EMG is applied to the study of skeletal muscle. The skeletal muscle tissue is attached to the bone and its contraction is responsible for supporting and moving the skeleton. The contraction of skeletal muscle is initiated by impulses in the neurons to the muscle and is usually under voluntary control. Skeletal muscle fibers are well-supplied with neurons for its contraction. This particular type of neuron is called a "motor neuron" and it approaches close to muscle tissue, but is not actually connected to it. One motor neuron usually supplies stimulation to many muscle fibers.

The human body as a whole is electrically neutral; it has the same number of positive and negative charges. But in the resting state, the nerve cell membrane is polarized due to differences in the concentrations and ionic composition across the plasma membrane. A potential difference exists between the intra-cellular and extra-cellular fluids of the cell. In response to a stimulus from the neuron, a muscle fiber depolarizes as the signal propagates along its surface and the fiber twitches. This depolarization, accompanied by a movement of ions, generates an electric field near each muscle fiber. An EMG signal is the train of Motor Unit Action Potential (MUAP) showing the muscle response to neural stimulation. The EMG signal appears random in nature and is generally modeled as a filtered impulse process where the MUAP is the filter and the impulse process stands for the neuron pulses, often modeled as a Poisson process (3). Figure Figure11 shows the process of acquiring EMG signal and the decomposition to achieve the MUAPs.

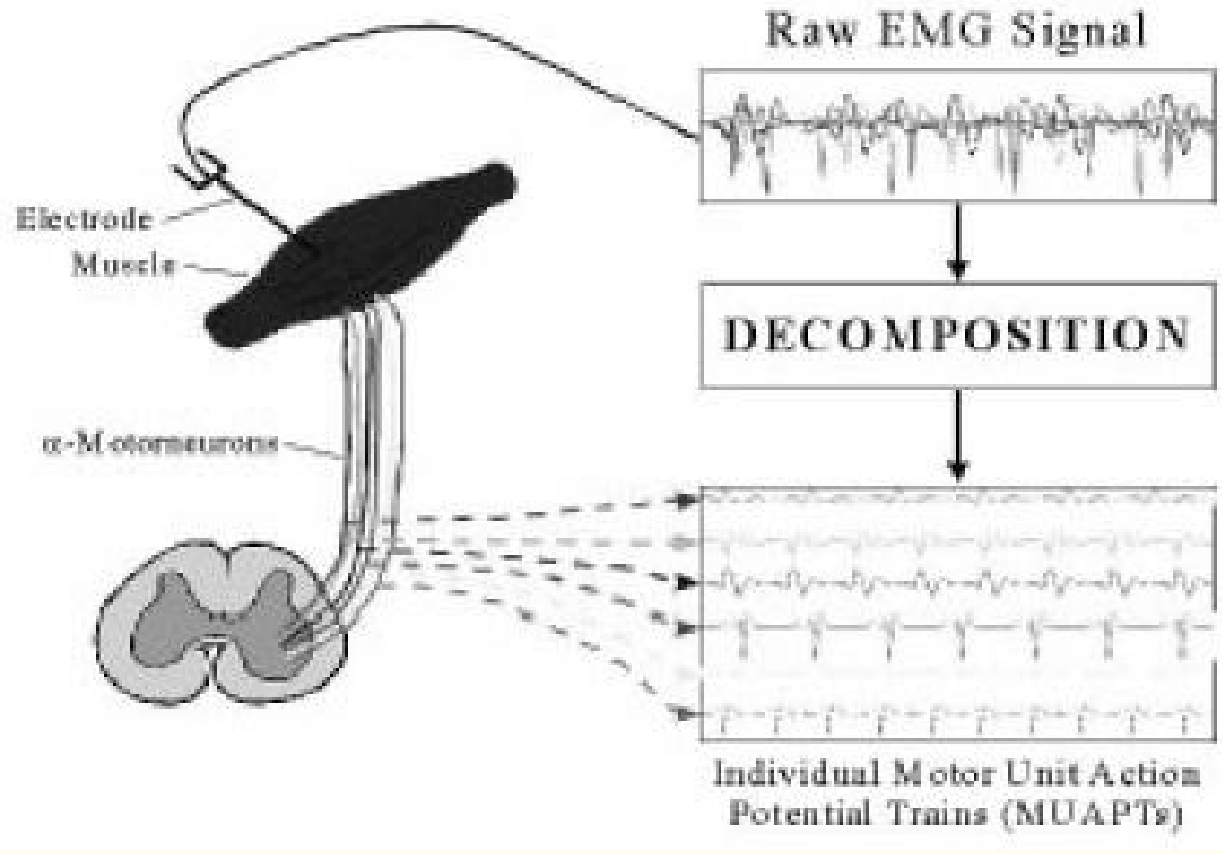


Fig. 1 EMG signal and decomposition of MUAPs.

Electrical noise and factors affecting EMG signal

The amplitude range of EMG signal is 0-10 mV (+5 to -5) prior to amplification. EMG signals acquire noise while traveling through different tissue. It is important to understand the characteristics of the electrical noise. Electrical noise, which will affect EMG signals, can be categorized into the following types:

1. *Inherent noise in electronics equipment*: All electronics equipment generate noise. This noise cannot be eliminated; using high quality electronic components can only reduce it.
2. *Ambient noise*: Electromagnetic radiation is the source of this kind of noise. The surfaces of our bodies are constantly inundated with electric-magnetic radiation and it is virtually impossible to avoid exposure to it on the surface of earth. The ambient noise may have amplitude that is one to three orders of magnitude greater than the EMG signal.
3. *Motion artifact*: When motion artifact is introduced to the system, the information is skewed. Motion artifact causes irregularities in the data. There are two main sources for motion artifact: 1) electrode interface and 2) electrode cable. Motion artifact can be reduced by proper design of the electronics circuitry and set-up.

4. *Inherent instability of signal:* The amplitude of EMG is random in nature. EMG signal is affected by the firing rate of the motor units, which, in most conditions, fire in the frequency region of 0 to 20 Hz. This kind of noise is considered as unwanted and the removal of the noise is important.

The factors that mainly affect the EMG signal can also be classified. This kind of classification is set so that EMG signal analysis algorithms can be optimized and equipments can be designed in a consistent manner. Factors affecting EMG signal falls into three basic categories:

1. *Causative Factors:* This is the direct affect on signals. Causative factors can be divided into two classes:
 - i. *Extrinsic:* This is due to electrode structure and placement. Factors like area of the detection surface, shape of electrode, distance between electrode detection surface, location of electrode with respect to the motor points in the muscle, location of the muscle electrode on the muscle surface with respect to the lateral edge of the muscle, orientation of the detection surfaces with respect to the muscle fibers mainly have an effect on EMG signal.
 - ii. *Intrinsic:* Physiological, anatomical, biochemical factors take place due to number of active motor units, fiber type composition, blood flow, fiber diameter, depth and location of active fibers and amount of tissue between surface of the muscle and the electrode.
2. *Intermediate Factors:* Intermediate factors are physical and physiological phenomena influenced by one or more causative factors. Reasons behind this can be the band-pass filtering aspects of the electrode alone with its detection volume, superposition of action potentials in the detected EMG signal, conduction velocity of the action potential that propagate along the muscle fiber membrane. Even crosstalk from nearby muscle can cause Intermediate Factors.
3. *Deterministic Factors:* These are influenced by Intermediate Factors. The number of active motor units, motor firing rate, and mechanical interaction between muscle fibers have a direct bearing on the information in the EMG signal and the recorded force. Amplitude, duration, and shape of the motor unit action potential can also be responsible.

The maximization of the quality of EMG signal can be done by the following ways:

1. The signal-to-noise ratio should contain the highest amount of information from EMG signal as possible and minimum amount of noise contamination.
2. The distortion of EMG signal must be as minimal as possible with no unnecessary filtering and distortion of signal peaks and notch filters are not recommended.

During the EMG signal processing, only positive values are analyzed. When half-wave rectification is performed, all negative data is discarded and positive data is kept. The absolute value of each data point is used during full-wave rectification. Usually for rectification, full-wave rectification is preferred.

EMG signal detection

Precise detection of discrete events in the sEMG (like the phase change in the activity pattern associated with the initiation of the rapid motor response) is an important issue in the analysis of the motor system. Several methods have been proposed for detecting the on and off timing of the muscle.

The most common method for resolving motor-related events from EMG signals consists of visual inspection by trained observers. The “single-threshold method,” which compares the EMG signal with a fixed threshold, is the most intuitive and common computer-based method of time-locating the onset of muscle contraction activity (6). This technique is based on the comparison of the rectified raw signals and an amplitude threshold whose value depends on the mean power of the background noise (7). The method can be useful in overcoming some of the problems related to visual inspection. However, this kind of approach is generally not satisfactory, since measured results depend strongly on the choice of threshold. This kind of method often rely on criteria that are too heuristic and does not allow the user to set independently the detection and false alarm probabilities (8). In “single-threshold method,” the relationship between the probability of detection P_{dk} and the probability P_γ that a noise sample is above the threshold γ is given by equation 2.

$$P_{dk} = \exp\left(\frac{\ln(P_\gamma)}{SNR/10}\right) \quad (2)$$

In 1984, Winter (9) observed that this approach is generally unsatisfactory, since it strongly depends on the choice of the threshold. To overcome the “single-threshold” problems, Bornato *et al.* (8) introduced “double-threshold detection” method in 1998. Double-threshold detectors are superior to single-threshold because they yield higher detection probability. Double-threshold detectors allow the user to adopt the link between false alarm and detection probability with a higher degree of freedom than single-threshold. The user can tune the detector according to different optimal criteria, thus, adapting its performances to the characteristics of each specific signal and application (8).

The sEMG signal recorded during voluntary dynamic contractions may be considered as a zero-mean Gaussian process $s(t)\in N(0,\sigma_s)$ modulated by the muscle activity and corrupted by an independent zero-mean Gaussian additive noise $n(t)\in N(0,\sigma_n)$. If the probability of detection is P_d then the double-threshold method is given by equation 3.

$$P_d = \sum_{k=r_o}^m \binom{m}{k} P_{dk}^k (1 - P_{dk})^{m-k} \quad (3)$$

The behavior of the double-threshold detector is fixed by the parameters: the threshold r_o , and the length of the observation window, m . Their values are selected to minimize the value of the false-alarm probability and maximize P_d for each specific signal-to-noise ratio (SNR) (8). In 2004, Lanyi and Adler (10) found that the double-threshold method proposed by Bornato is complex and computationally expensive, requiring a whitening of the signal. It is also not very sensitive. Lanyi

and Andy proposed a new algorithm based on the double-threshold method that is more sensitive, stable, and efficient with decreased computation cost. For specific applications, besides the accuracy in the detection, the speed of the algorithm can be an important consideration. Algorithms with high computation time are unsuitable for online detection. One specific drawback to the method of Bornato *et al.* (8) is the detection probability to be maximum when P_{fa} is fixed, the second threshold has to be chosen as equal to "1." The second threshold is fixed during detection, which implies that the double-threshold detector actually becomes single-threshold detector. This method does not require the signal-whitening step, which is needed previously. The whitening process takes a lot of computation time. Moreover, the whitening process reduces probability of the signal. This feature will cause the detection to miss a part of activation interval. The methods proposed by Lanyi and Adler (10) provides a fast and more reliable muscle on-off detection. Table [Table11](#) shows the comparison of the different detection methods at a glance based on research works by Merlo and Farina (11) in 2003.

Table 1

Comparison of 3 main EMG detection methods.

	SNR(db)								
	2		4		6		8		
Method	Bias	Std	Bias	Std	Bias	Std	Bias	Std	Remark
Improved method (11)	-39	26	-22	25	-12	22	-3	17	Best
Double threshold (8)	41	68	21	69	12	47	0	53	Good
Single threshold (11)	55	154	67	147	62	135	72	139	Worse

Applications of EMG

EMG signals can be used for variety of applications like clinical/biomedical applications, EHW chip development, human machine interaction, etc. Clinical applications of EMG as a diagnostics tool can include neuromuscular diseases, low back pain assessment, kinesiology and disorders of motor control. EMG signals can be used to develop EHW chip for prosthetic hand control. Grasp recognition ([73](#)) is an advanced application of the prosthetic hand control.

EMG can be used to sense isometric muscular activity (type of muscular activity that does not translate into movement). This feature makes it possible to define a class of subtle motionless gestures to control interface without being noticed and without disrupting the surrounding environment. The device for this purpose includes a high input impedance amplifier connected to electrodes, an anti-aliasing filter, a microcontroller to sample and process the EMG signal, and a Bluetooth communication module to transmit the processing results. When activation is detected, the controller sends a signal wirelessly to the main wearable processing unit, such as a mobile phone or PDA. Using EMG, the user can react to the cues in a subtle way, without disrupting their environment and without using their hands on the interface. The EMG controller does not occupy the user's hands, and does not require them to operate it; hence it is "*hands free*" ([74](#)).

Interactive computer gaming offers another interesting application of bio-signal based interfaces. The game system would have access to heart rate, galvanic skin response, and eye movement signals, so the game could respond to a player's emotional state or guess his or her level of situation awareness by monitoring eye movements. An interactive game character could respond to a user who stares or one who looks around, depending on the circumstances. This use of eye tracking is easier than using the eyes as a precision pointing device, which is difficult because the eyes constantly explore the environment and do not offer a stable reference for a screen pointer. To provide more fun and strategies, there are usually two styles of attack possible in fighting games. One is the weak attack and the other is the strong attack. Common input devices for fighting action games are the *joypad* and *joystick*. These use a stick to move the character and a button to make a certain type of attack, for example, a punch or kick. To make a strong attack the user has to input a complex key sequence that makes that motion difficult to invoke, thereby achieving a balance between two types of attack. Though those devices are cheap and easy to use, they have disadvantages. These interfaces are not intuitive for human fighting movement control, and the user has much to memorize, such as the meaning of the button and the input sequence for a strong attack motion. A human-computer interface device designed for a fighting action game, "*Muscleman*," has been developed by D. G. Park and H. C. Kim in Korea. The game characters are usually depicted as making an isometric contraction of their arms as an expression of power concentration to make a strong attack like a fireball ([75](#)).

To measure the force of the isometric muscle contraction, a surface EMG was used. Moreover, to obtain more precise information about the user's forearm movement, the gaming system is installed with an accelerometer. By analyzing acceleration data record obtained from the accelerometer, it is possible to know which direction the forearm is moving. Furthermore, the classification of attack movement in cases such as whether the motion was a straight punch motion or an upper cut motion is possible. Wireless transmission is adopted so as not to disturb the user's motion. By adopting wireless transmission, the stage of a game can be extended virtually with no limits in space. Figure [Figure99](#) shows the system block diagram of "*Muscleman*."

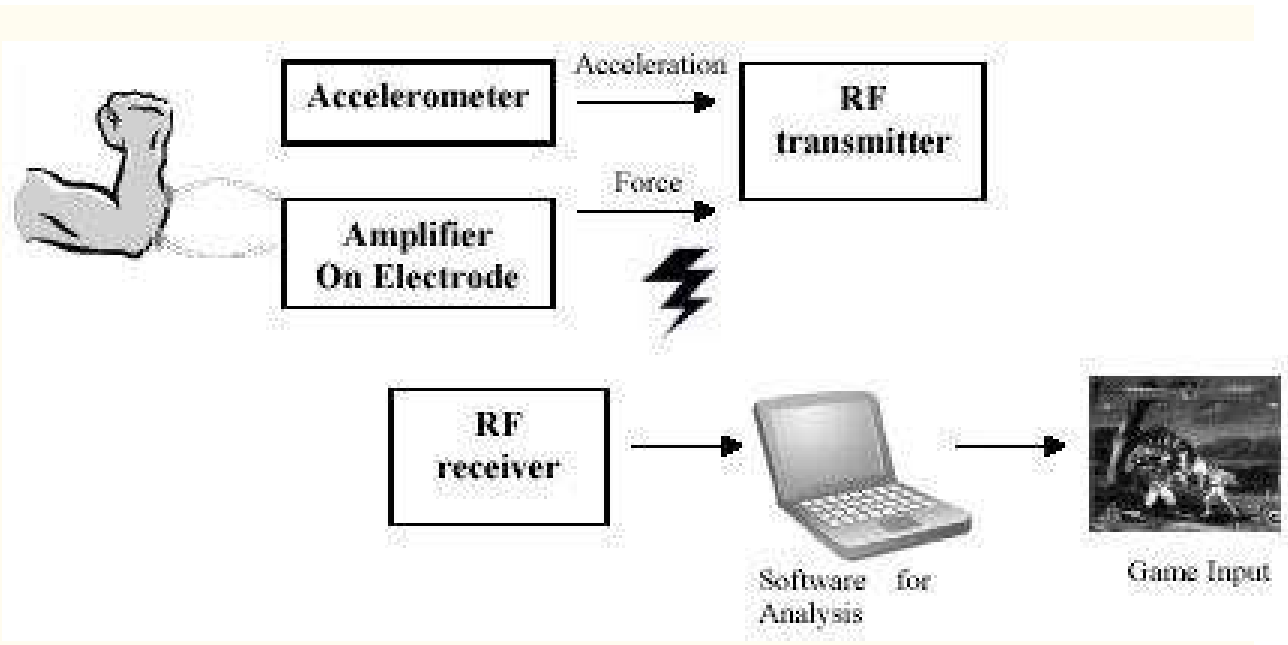


[Fig. 9](#) System block diagram of "Muscleman."